ELSEVIER

Diamond and Related Materials 10 (2001) 260–264

DIAMOND AND RELATED MATERIALS

www.elsevier.com/locate/diamond

Field emission from nano-cluster carbon films

W.I. Milne*, A. Ilie, J.B. Cui, A. Ferrari, J. Robertson

Department of Engineering, Cambridge University, Cambridge CB2 1PZ, UK

Abstract

Field emission has been reported to occur at much lower fields in carbon based thin film systems than from any other material systems. The emission has been shown to depend on the various material parameters, but whichever carbon based system is used, it is found that emission occurs at localised sites rather than uniformly over the entire surface. Carbon films with mixed sp^3/sp^2 bonding, like nanocrystalline diamond and nanocluster graphitic films emit at lower fields with a higher emission site density than single-phase films. The sp^2 cluster size in any carbon film can be altered during deposition, but it is easier to control nanocluster size by post-deposition annealing. Annealing increases the sp^2 cluster size embedded in a sp^3 matrix until the sp^3 matrix disappears completely and the film transforms into nanocrystalline graphite. To distinguish the effects of the sp^2 cluster size from other material parameters, a series of different carbon films were annealed post-deposition and the sp^2 cluster size was measured using visible Raman. Field emission was then measured at a vacuum of 10^{-8} mbar on all films using a parallel plate configuration. It was found that the field emission for all films tested depended upon the clustering of the sp^2 phase and this effect dominates the effects of the other parameters, such as chemical composition, surface termination, sp^3 content or conductivity. The optimum size of the sp^2 was of the order of 1 nm for all systems tested. We believe that field emission occurs form the localised conducting, predominantly sp^2 bonded regions, which provideds the large field enhancement required for effective emission.

Keywords: Carbon-based cathode; Field emission displays; Electron emission

1. Introduction

Over the past few years, there has been an increasing interest in using carbon based films as the cathode material in tip free field emission displays (FEDs). Various carbon-based cold cathodes, including diamond [1], nano-diamond [2,3], diamond-like carbon (DLC) and tetrahedral amorphous carbon (ta-C) [4,5], carbon nanotubes [6–8] and nanocluster carbon [9,10], have all been shown to emit electrons at reasonably low fields. However, the exact mechanism of electron emission from these carbon-based cold cathodes is yet to be fully understood [11]. These materials have been grown using hot filament CVD [1,8], microwave plasma CVD [7], plasma-assisted DC discharge [10] and cathodic arc techniques [5,9,20].

Amongst these, the cathodic arc process offers the unique opportunity of growing any form of carbon from diamond-like to graphite-like and various intermediate stage materials, such as tetrahedral amorphous carbon (ta-C), hydrogenated ta-C and nanoclusters, all at room temperature. ta-C, with up to approximately 85% sp^3 bonding, can be grown using the cathodic arc process. The sp^3/sp^2 ratio of the ta-C films can be altered by changing the incident ion energy by applying a negative bias to the substrate [12]. Smooth carbon films with inclusions of fullerene, nano particles and nanotubes grown using the arc process have been reported [13] and nanocluster carbon films with coral-like structures have also been produced [9]. Thus, various types of material can be grown using the same arc process by varying the system configuration and deposition

* Corresponding author. Tel.: +44-1223-332757; fax: +44-1223-766207.

E-mail address: wim@eng.cam.ac.uk (W.I. Milne).

0925-9635/01/$ - see front matter
PII: S0925-9635(00)00479-9

Table 1
Potential applications and their field emission requirements

	Current density	Low field	Site density	Current stability	Energy width
Microwave amp	**			**	
FE display		*	**	**	*
Power switch	**	**			
FE gun	***			**	**
Lithography		*	**	*	*

Table 2
Emission properties of various carbon films

	Current density	Low field	Site density	Current stability	Deposition temperature
Diamond				*	
Nano-diamond	*	**	**	**	
Diamond-like		*			**
Nano-structured carbon	*	**	**	**	**
Nanotubes	***	**	**	*	(*)

parameters. More recently, the arc process has been used to synthesise large quantities of carbon clusters [14]. Higher fullerenes have also been produced [15]. Field emission at very low fields has been reported for many of these films [16–18].

In fact, there are several potential applications for field emission in electronic devices. Each device requires a slightly different set of material parameters. For example, it is now recognised that a practical flat panel field emission display requires not only low threshold fields, but also a high emission site density of the order of $10^6/cm^2$. None of the above films have been found to have sufficient site densities to be suitable for FED applications, with the exception of nanocluster 'coral-like' films [9], which exhibit high emission site densities at approximately 20 V/μm field. Other potential applications and the requirements for each application are summarised in Tables 1 and 2 [18]. The use of carbon as the electron emitter in microwave amplifiers and in vacuum power switches is becoming increasingly of interest and their use in novel parallel e-beam lithography systems is currently being investigated as part of a Framework V EC project in collaboration with Thomson CSF and the Fraunhoffer Insitute [19].

We have previously reported a series of experiments on as-grown ta-C films. Emission was shown to be a function of ion energy during deposition, and samples with ~85% sp^3 bonding were shown to emit electrons with a threshold field of 10–20 V/μm. Nitrogen incorporated ta-C films containing nearly ~1% nitrogen have threshold fields as low as 2–5 V/μm. The threshold field is defined as that field at which a 1-$\mu A/cm^2$ current density is obtained. The effect of surface treatment on the emission properties of ta-C has also been investigated [5,17,19]. In this paper, we will now review the work carried on field emission from the various nano-cluster carbon materials produced in our laboratory. We used two methods to produce the films. By varying the deposition conditions in a FCVA system, a series of cluster carbon films was made and tested. However, in order to control the cluster size more precisely, several series of cluster carbon samples, with and without the addition of nitrogen and/or hydrogen, were produced by post-deposition annealing [23] and field emission as a function of sp^2 cluster size was investigated.

2. Experimental methods

The first set of films was produced using a typical filtered cathodic vacuum arc system, a schematic diagram of which is shown in Fig. 1. As mentioned in a previous paper [5], mirror smooth films of ta-C have been grown in this deposition chamber (region A) where macroparticles have been successfully filtered out. Nanocluster carbon films and fibrous type films, on the other hand, can be grown in region B, which is within line of sight of the graphite cathode. The films were deposited in a nitrogen/helium atmosphere. Nitrogen flow was held constant to produce nitrogen partial pressures of 10^{-3} and 10^{-4} torr, respectively, and the helium partial pressure was altered to produce a variety of film types. After our preliminary results on such films, a dedicated unfiltered cathodic arc system was commissioned to deposit subsequent films.

However, in order to study the effect of sp^2 cluster size on field emission behaviour in some detail, we

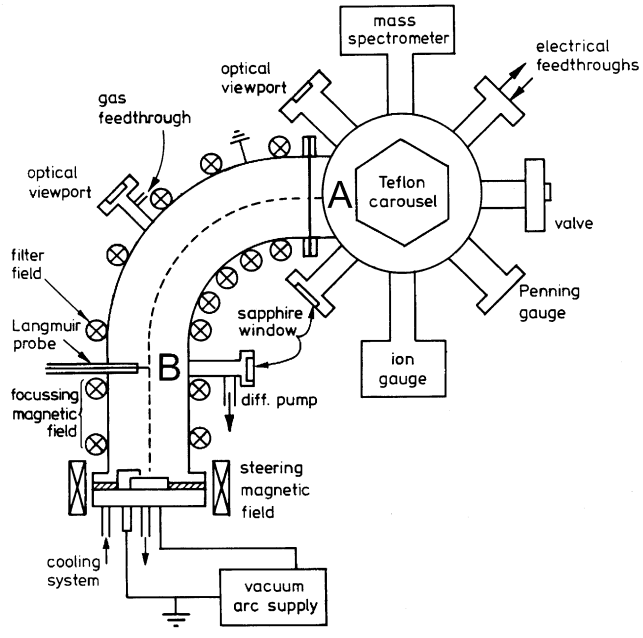

Fig. 1. Schematic of cathodic arc deposition system.

carried out a series of post-deposition annealing experiments to accurately control the sp^2 cluster size within the sp^3 matrix. Annealing increases the size of the sp^2 clusters until the sp^3 phase completely disappears and the film transforms into nanocrystalline graphite. In order to differentiate between the effects of other factors such as H incorporation, N incorporation, bonding configuration or surface termination, we studied a whole series of carbon films with and without hydrogen and nitrogen incorporation.

a-C:H films with bandgaps of, typically, 1.7 eV and a sp^2 content of the order of 35–40% were deposited by rf PECVD. Ta-C films with a sp^3 content of $\sim$85% were deposited in region A of our FCVA system, shown schematically in Fig. 1. Lightly N-doped ta-C films were deposited in the same system. Ta-C:H films were subsequently deposited in an electron cyclotron wave resonance system at an ion energy of 130 eV [22]. The films were annealed in vacuum of 10^{-6} mbar for 20 min up to 1000°C for the ta-C films and to 700°C for the a-C:H samples.

Films of approximately 30–50 nm thick were deposited onto heavily n-type doped Si (100). Field emission measurements have been carried out in a parallel plate configuration, where the cathode consists of the carbon films to be tested and the anode consists of either an ITO coated glass plate or a phosphor coated glass plate (for emission site density measurements) [5,21]. The I–V measurements were made with an anode–cathode spacing of either 85 or 100 μm under a vacuum of 10^{-8} mbar. The inter-electrode spacing was defined by spacers maintained outside the emission area to avoid any leakage paths or field enhancement at the edges. Most of the cluster carbon films emit upon the first application of an applied bias above a certain threshold level.

However, in some instances, e.g. for a-C:H, the films were subjected to a series of voltage ramps of increasing applied bias in order to initiate emission. A ramp rate of typically 1 V/s was used. We defined our threshold field as that necessary to produce an emission current density of 10^{-6} A/cm^2. The parallel plate configuration, of course, measures only the most emissive spots. Nevertheless, the clear trend that is observed in our data is difficult to explain if there is no relationship between field emission and structure.

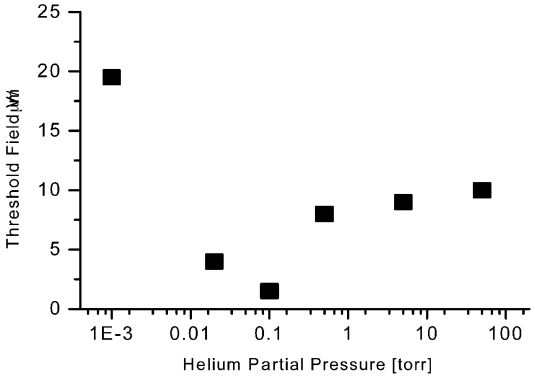

Fig. 2. Threshold field as function of He partial pressure at a nitrogen partial pressure of 10^{-3} torr.

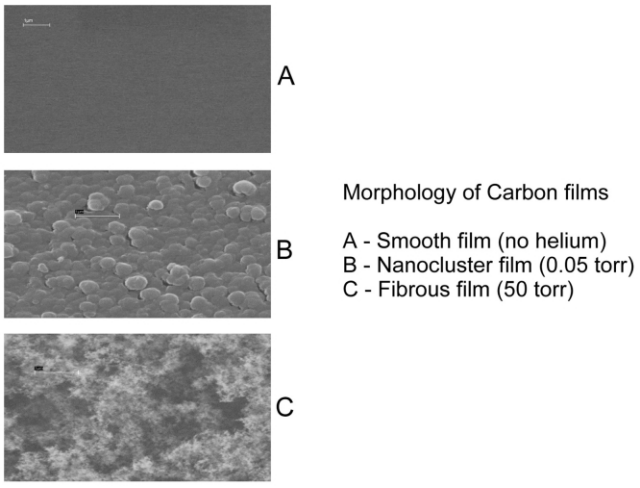

Fig. 3. Film morphology as a function of He partial pressure at 10^{-3} torr N partial pressure.

Fig. 2 shows the threshold field as a function of helium partial pressure for a constant nitrogen partial pressure of 10^{-3} torr. A similar trend is seen for films grown at a constant nitrogen partial pressure of 10^{-4} torr.

This shows that as the He partial pressure increases, the threshold field reduces and then increases as the pressure is further increased. The threshold field reaches a minimum of $\sim$1 V/μm at a He partial pressure of 0.1 torr. An SEM picture (Fig. 3) of the various materials grown in region B indicates how the surface morphology alters as a function of He partial pressure. There is a tendency for the clusters to coalesce as the He partial pressure increases. However, at 50 torr He partial pressure, the films become fibrous and the threshold field increases.

The initial increase in cluster size with increasing helium pressure may be due to the enhanced interaction between the carbon atoms in the presence of the helium atoms as it partly reduces the kinetic energy (K.E.) of the ions and also prevents them from diffusing away. This enhances the interaction between ions leading to cluster formation. The He ions and neutrals also impinge upon the carbon clusters and release their excess energy. This helps the surface mobility of the small clusters and with the addition of more carbon atoms, they coalesce to form bigger clusters. However, cluster size does not increase linearly with He partial pressure, and after a particular cluster size, the clusters do not further coalesce but instead the constant bombardment of the ions and neutrals leads to the formation of smaller clusters or even fibrous type growth.

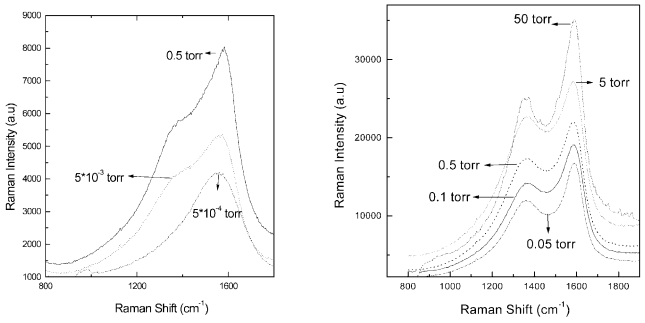

Fig. 4. Visible Raman spectra of nanocluster carbon films grown under varying helium partial pressures while maintaining a constant nitrogen partial pressure of (a) 10^{-4} torr and (b) 10^{-3} torr.

Visible Raman measurements were also carried out on the above samples and are shown in Fig. 4a,b for N partial pressures of 10^{-4} and 10^{-3} torr, respectively. Visible Raman is mainly sensitive to sp^2 sites and is a suitable method to study the evolution of the sp^2 phase within an sp^3 matrix. The presence of the Raman 'D' peak at 1350 cm^{-1} indicates that the sp^2 phase clusters into aromatic rings. As can be seen from the figures, in the absence of any helium there is no 'D' peak present, but as the helium partial pressure increases, the 'D' peak becomes increasingly significant. It is obvious from the above figures that within the larger carbon cluster seen in the SEM pictures, smaller sp^2 clusters are also forming. These preliminary results on emission from clustered films encouraged us to investigate in detail the effects of this sp^2 cluster formation of field emission.

Tuinstra and Koening [25] showed that there is a simple relationship between the in-plane correlation length L_a of the sp^2 clusters and the intensity ratio of the 'D' and 'G' peaks, $I(D)/I(G)$. They showed that for $L_a > 2$ nm, $I(D)/I(G)$ decreases as $1/L_a$. Recently, Ferrari and Robertson [24] have shown from their work on ta-C films that the dependence of $I(D)/I(G)$ for $L_a < 2$ nm is somewhat different. They showed that as the D peak does not exist for as-grown ta-C, then L_a must equal zero at this point where $I(D)/I(G)$ also

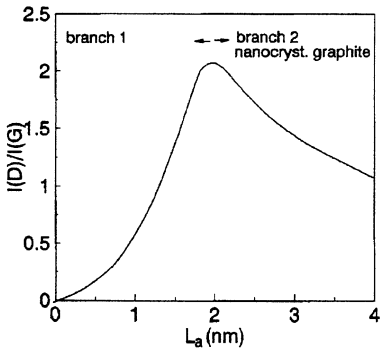

Fig. 5. Correlation between $I(D)/I(G)$ and in-plane correlation length of sp^2 clusters [23].

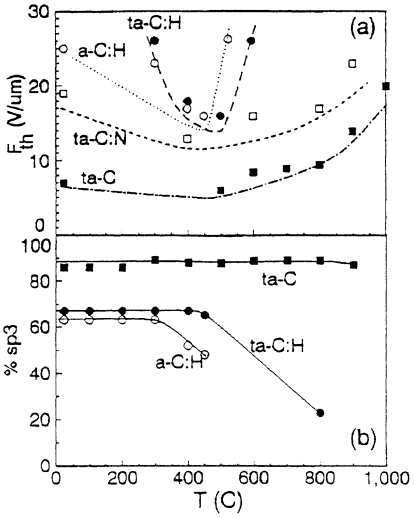

Fig. 6. (a) Variation of threshold Field and (b) sp^3 content as a function of annealing temperature [23].

equals zero. They hypothesised, therefore, that as L_a increases, then so must $I(D)/I(G)$. The exact dependence is debatable, but since the ratio depends upon the size of the clusters they have chosen a dependence on L_a^2, as shown in Fig. 5. $I(D)/I(G)$ is found by using a Breit–Wigner–Fano lineshape for the G peak and a Lorentzian for the D peak.

Fig. 6a shows the effect of annealing temperature on E_{th}. In all systems measured, the threshold field passes through a minimum before increasing again. Fig. 6b shows the sp^3 fraction (measured by EELS) as a function of the annealing temperature. The common behaviour for all samples shown in these figures indicate that it is not the chemical bonding to H or N, the surface termination nor the sp^3 content of the films that primarily determines the emission behaviour.

In order to study the effects of sp^2 cluster size on emission, the visible Raman spectrum for each sample was then measured and using branch 1 from Fig. 6, a measure of cluster size can be estimated and plotted vs. threshold field, as shown in Fig. 7.

As can be seen, there is an optimum size of cluster for each system where the threshold field is a mini-

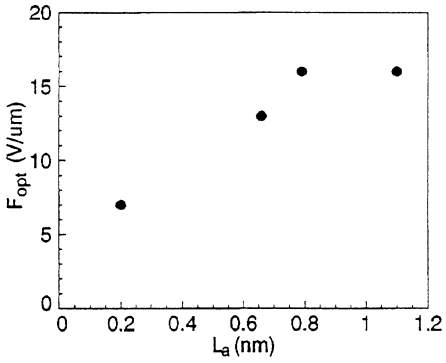

Fig. 7. Dependence of threshold field on L_a [23].

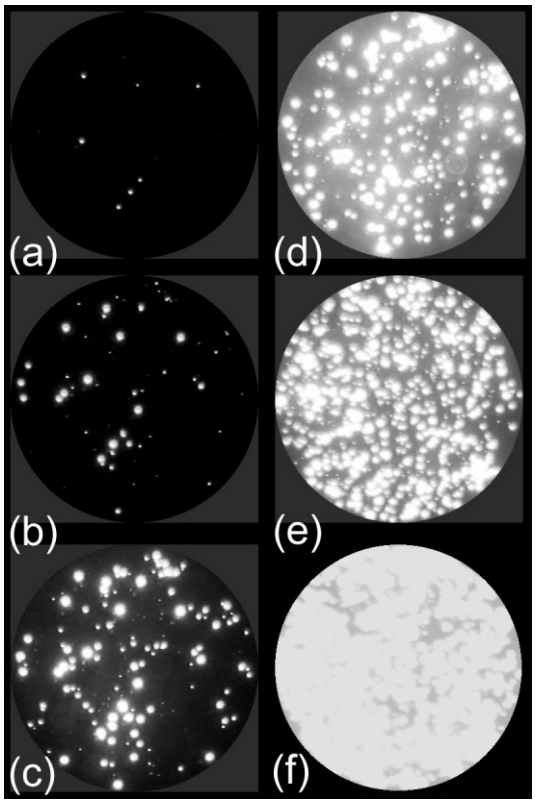

Fig. 8. Emission site density as a function of applied field: (a) 4; (b) 6; (c) 8; (d) 11; (e) 15; and (f) 20 V/μm. Each image is 1 cm in diameter.

mum. Each system has an optimum sp^2 cluster size of the order of 1 nm. The figure also shows that the threshold increases strongly in all systems when the sp^3 matrix disappears and the material tends towards the nanocrystalline graphite phase at $L_a \sim 2$ nm. This emphasises the need for both sp^2 and sp^3 phases to provide good emission.

In order for the cluster material to be useful as an emitter, for most applications the emission site density must also be high. Also, although the annealing experiments provide us with a detailed understanding of the emission behaviour, it will be necessary to produce our cluster films without recourse to post-deposition annealing. The next figure, Fig. 8, shows site density as a function of the applied field for as-grown cluster samples produced in our modified arc system. These show the sites in the cluster carbon that have sufficient current density to stimulate the phosphor and do not represent all possible emission sites.

3. Conclusions

The field emission in cluster carbon films has been measured as a function of sp^2 cluster size. The sp^2 cluster size was varied by post-deposition annealing of a series of different DLC films. Cluster films have also been produced in a modified cathodic arc deposition system. An improvement of both site density and reduction in threshold field has been obtained by optimising the cluster size. Further optimisation of the deposition technique is on-going in order to produce optimum cluster size without recourse to post-deposition annealing.

References

[1] C. Wang, A. Garcia, D.C. Ingram, M.E. Kordesch, Electron Lett. 27 (1991) 1459.
[2] A.A. Talin, L.S. Pan, K.F. McCarty, H.J. Doerr, R.F. Bunshah, Appl. Phys. Lett. 69 (1996) 3842.
[3] W. Zhu, G.P. Kochanski, S. Jin, L. Seibles, J. Vac. Sci. Technol. B 14 (1996) 2060.
[4] G.A.J. Amaratunga, S.R.P. Silva, Appl. Phys. Lett. 68 (1996) 2529.
[5] B.S. Satyanarayana, A. Hart, W.I. Milne, J. Robertson, Appl. Phys. Lett. 71 (1997) 1430.
[6] W.A. de Heer, A. Chatelain, D. Ugrate, Science 270 (1995) 1179.
[7] O.M. Kuttel, O. Groening, C. Emmenegger, L. Schlapbach, Appl. Phys. Lett. 73 (1998) 2113.
[8] Y. Chen, S. Patel, Y. Ye, D.T. Shaw, L. Guo, Appl. Phys. Lett. 73 (1998) 2119.
[9] B.F. Coll, J.E. Jaskie, J.L. Markham, E.P. Menu, A.A. Talin, P. von Allmen, MRS. Symp. Proc. 498 (1998) 185.
[10] O.N. Obraztsov, A.P. Volkov, I.Y.u. Pavlovsky, JETP Lett. 68 (1998) 59.
[11] J. Robertson, J. Vac. Sci. Technol. B 17 (1999) 659.
[12] P.J. Fallon, V.S. Veeraswamy, C.A. Davis et al., J. Phys. Rev. B 48 (1993) 4777.
[13] G.A.J. Amaratunga, M. Chhowalla, C.J. Kiely, I. Alexandrou, R.A. Aharonov, R. Devenish, Nature 383 (1996) 321.
[14] W. Kratschmer, L.D. Lamb, K. Fostiropoulous, D.R. Hoffman, Nature 347 (1990) 354.
[15] F. Diederich, R. Ettl, Y. Rubin et al., Science 252 (1991) 548.
[16] S. Iijima, Nature 354 (1991) 56.
[17] W.I. Milne, J. Robertson, B.S. Satyanarayana, A. Hart, Int. J. Modern Phys. B 14 (2–3) (2000) 301–307.
[18] J. Robertson, Proc. of MRS Symposium Vol 621 (2000).
[19] NANOLITH, EC Framework V project No IST 1999–11806.
[20] V.S. Veerasamy, J. Yuan, G.A.J. Amaratunga et al., Phys. Rev. B. 48 (1993) 17954.
[21] A. Hart, B.S. Satyanarayana, J. Robertson, W.I. Milne, Appl. Phys. Lett. 74 (1999) 594.
[22] N.A. Morrison, S. Muhl, S.E. Rodil et al., Phys. Stat. Solidi, A 172 (2000) 79.
[23] A. Ilie, A.C. Ferrari, T. Yagi, J. Robertson, Appl. Phys. Lett. 76 (18) (2000) 2627.
[24] A.C. Ferrari, J. Robertson, J. Phys. Rev. B 61 (2000) 14095.
[25] F. Tuinstra, J.L. Koening, J. Chem. Phys. 58 (1970) 1126.